



# Effects of a Topical Anti-aging Formulation on Skin Aging Biomarkers

by ALAN D. WIDGEROW, MBBCH, MMED, FCS, FACS; MARY E. ZIEGLER, PhD; JOHN A. GARRUTO, BS; and MICHAELA BELL, BS, MBA

All authors are with ALASTIN Skincare in Carlsbad, California. Drs. Widgerow and Ziegler are also with the Center for Tissue Engineering (CTE) at University of California Irvine in Irvine, California.

*J Clin Aesthet Dermatol.* 2022;15(8):E53–E60.

**OBJECTIVE:** Following previous clinical trials, an antiaging product (Restorative Skin complex [RSC]; Alastin Skin Care Carlsbad, a Galderma company), was investigated for its effects on Klotho gene regulation, telomere length, and histological biopsy changes to provide a comprehensive picture of the mechanism and efficacy of its anti-aging effect. **METHODS:** Neonatal human fibroblasts were used for telomere length studies to examine the effect of the full RSC formulation and the amino acid components Tripeptide-1 and Hexapeptide-12 (TriHex™) on these cellular aging mechanisms. In addition, RNA sequencing was conducted using human keratinocytes specifically investigating Klotho and related genes. This was supplemented by a clinical study using biopsy samples. **RESULTS:** TriHex™ significantly upregulated the Klotho gene and related FGF23, FGFR1 and FOXO3B anti-aging genes. Significant telomere shortening reduction over control was demonstrated with the RSC formulation at four weeks and with TriHex™ at six weeks for all percentiles tested. Previous clinical studies demonstrated that the use of the antiaging regimen for 12 weeks produced a statistically significant improvement in scores for all evaluated parameters. Restaining of previous biopsy blocks from the clinical trial revealed positive ECM changes, stimulation of collagen, fibrillin, CD44 and elastin. **LIMITATIONS:** The study was limited by a relatively small numbers of patients in the clinical trial and the non-competitive nature of the trial. **CONCLUSION:** RSC anti-aging formulation and its TriHex™ components demonstrated significant reduction in telomere shortening, upregulation of Klotho and FOXO3 genes and biopsy validation of anti-aging efficacy. This new science supplements previous trials that demonstrated clinical efficacy of the formulation **KEYWORDS:** Klotho gene, Telomere, anti-aging, elastin, fibrillin

Skin aging is a natural process through wear and tear on a constant basis but is profoundly exaggerated by exposure to the sun. This manifests as gradually advancing loss of elasticity, fine lines, pigmentation, and a slowed turnover of regenerating cells.<sup>1,2</sup> These regenerative cells are bathed in an extracellular matrix (ECM) that provides nutrients to the cells and promotes communication between cells and important proteins like collagen. With time and sun exposure, breakdown products begin to accumulate in the ECM, interfering with nutrient exchange and communication creating a shortage of collagen and elastin, decreased skin thickness, and loss of elasticity.<sup>1,3</sup>

New approaches to this problem have concentrated on an effort to recycle the ECM, removing old accumulated fragments of protein resulting from sun damage and aging and replacing these with newly created proteins (i.e., collagen and elastin) that result in regenerated skin.<sup>2</sup> The newer active agents that achieve these effects include specially identified peptides (i.e., small protein fragments) recognized by the body and highly efficient at creating these changes. Together with active extracts from plant botanicals, synergistic combinations of new formulations provide

exciting new avenues for combatting and managing the skin aging process.<sup>2,4</sup>

In addition to these profound ECM changes, genetic and epigenetic influences play a significant role in skin aging. Klotho is the first documented aging suppressor gene in mammals that is purported to delay aging.<sup>5</sup> The gene codes a membrane protein that shares sequence similarity to a beta glycoside enzyme. The extracellular domain of the Klotho protein is split, and the fragment that circulates in the blood is a hormone that represses intracellular signals of insulin and insulin-like growth factor (IGF1).<sup>5</sup> Inhibiting this insulin signaling pathway is one of the evolutionarily conserved mechanisms for suppressing aging.<sup>5</sup> Overexpression of the Klotho gene was demonstrated to markedly alleviate the ultraviolet B (UVB)-induced damages to keratinocytes and significantly reverse the UVB-caused biomarker changes.<sup>6</sup>

Stem cells, in combination with anti-aging genes, provide protection against the aging process. Increased wear and tear of the stem cells, as well as Klotho deficiency, results in increased cellular damage and accelerated aging.<sup>7</sup> When stem cells divide, their telomeres shorten, and

**FUNDING:** Funding for this study was provided by ALASTIN Skincare, Inc., a Galderma Company.

**DISCLOSURES:** All authors are employees of ALASTIN Skincare, Inc.

**CORRESPONDENCE:** Alan D. Widgerow MBBCh, MMed, FCS, FACS; Email: awidgerow@alastin.com

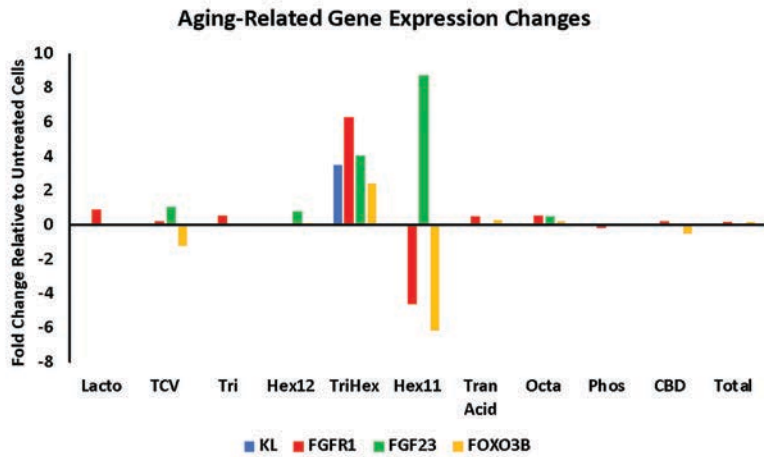


**FIGURE 1.** TriHex™ upregulates aging-related gene expression in keratinocytes. Human keratinocytes were treated with Lactoferrin (Lacto), TCVRRAF (amino acid sequence extracted from Lactoferrin) (TCV), Tri-peptide-1 (Tri), Hexapeptide-12 (Hex12), TriHex™ combination (TriHex™), Hexapeptide-11 (Hex11), Tranexamic acid 5% (Tran acid), Octapeptide, a proprietary peptide designed by R&D at Alastin (Octa), Phosphatidylserine (Phos), Cannabidiol (CBD), or left untreated for 24 hours. Then, RNA was extracted, and RNA-seq was performed. The data are presented as the fold-change in gene expression relative to the non-treated cells.

KL: Klotho; FGFR1: Fibroblast Growth Factor Receptor 1; FGF23: Fibroblast Growth Factor 23; FOXO3B: Forkhead box O3

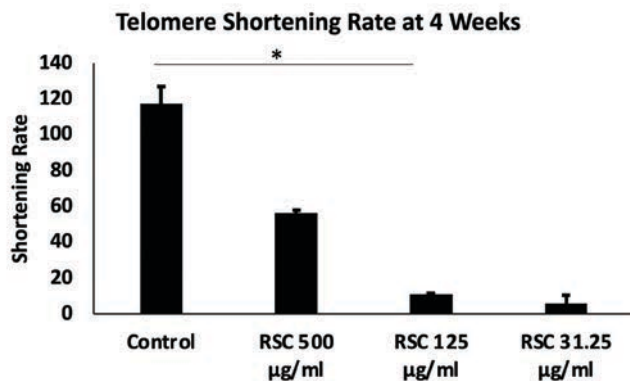


**FIGURE 2.** RSC protects against telomere shortening in fibroblasts. Human primary adult fibroblasts were treated with the RSC formulation at 500, 125, and 31.25 µg/mL for four weeks. The TAT assay was conducted to determine the telomere lengths. Then, the telomere shortening rate was determined by the following formula: median telomere length (initial-final)/population doubling. The values were compared, and the data represent the mean ± SD. \*  $p < 0.05$

cells stop dividing and die. Telomerase prevents this decline in stem cells by lengthening telomeres, but a decrease in this enzyme has been reported in the aging process.<sup>7</sup>

Finally, when validating the proof of concept of an agent or formulation purported to limit or reverse the signs of aging elucidated above, histological changes are still the gold standard in assessing the efficacy of such formulations. The molecular changes taking place, particularly within the ECM, appear to pre-empt the physical changes observed when using these formulations.

In an effort to test the efficacy of such a product (Restorative Skin complex [RSC], Alastin Skincare, a Galderma company; Carlsbad, California) as an addition to previous traditional clinical trials,<sup>2</sup> we have investigated the effects on Klotho gene regulation, telomere assessment, and histological biopsy changes to provide a comprehensive picture of the mechanism and efficacy of the anti-aging effect of RSC.

## METHODS

**Cell culture.** Human adult keratinocytes

were purchased from Zen-Bio (Durham, North Carolina) and cultured in keratinocyte media (Zen-Bio). The cells were maintained at 37°C in a 5% CO<sub>2</sub> incubator. These cells were used for RNA sequencing.

Primary adult or neonatal human fibroblasts were established under standard culture conditions. The cells were seeded in a fibroblast medium kit (Innoprot; Bizkaia, Spain) and were maintained in an incubator with an atmosphere of 5% CO<sub>2</sub>/95% air at 37°C. These cells were used for the MTT assay, proliferation, and telomere length studies.

**Cell treatments for RNA-seq.** The keratinocytes were seeded into 48-well plates and left for 48 hours. Then, the cells were treated with the following compounds for 24 hours: Lactoferrin (500 µg/mL), TCVRRAF (100 µg/mL) (amino acid sequence extracted from Lactoferrin), Tri-peptide-1 (2.9 µg/mL), Hexapeptide 12 (2.9 µg/mL), TriHex™ combination (2.9 µg/mL), Hexapeptide 11 (100 µg/mL), Tranexamic acid 5% (500 µg/mL), Octapeptide, a proprietary peptide designed by R&D at Alastin (Alastin, a Galderma Company; Carlsbad California) (100 µg/mL), Phosphatidylserine (500 µg/mL), or Cannabidiol (CBD) (100 µg/mL). Untreated cells served as the negative control. The compounds were resuspended in the appropriate vehicle. Trihex technology (combination of Tripeptide-1 and Hexapeptide 12) is the peptide backbone of the RSC product. An array of compounds was tested to enable comparisons with the TriHex™ combination.

**RNA lysate preparation.** After 24 hours in the presence of the compounds, the cells were washed once with phosphate-buffered saline (PBS). Then, 100 µl of RNA Lysis Buffer (Takara Bio Cat Num 635013, "10X RNA lysis buffer", diluted to 1X) was added to the well.

The buffer was mixed thoroughly in the wells by trituration, and the resulting lysate was placed in an RNase free microcentrifuge tube and frozen immediately at -30°C.

**RNA-seq.** The RNA lysate samples were shipped frozen on dry ice to MedGenome (Foster City, California) for RNA extraction, library construction, and sequencing to 25M paired-end 100bp reads per sample. After obtaining the reads, the differentially expressed genes were analyzed using the Reactome Pathway.<sup>8</sup>

**MTT assay.** Primary adult or neonatal human fibroblasts were seeded in 96-well plates at

0.5x10<sup>4</sup> cells/plate and 0.35x10<sup>4</sup> cells/plate for the 72 hour and one-week treatments, respectively. The complete RSC formulation cream was used and dissolved in dimethyl sulfoxide (DMSO). Eight serial dilutions were prepared (500µg/mL, 250µg/mL, 125µg/mL, 62.5µg/mL, 31.25µg/mL, 15.62µg/mL, 7.8µg/mL, and 3.8µg/mL) to evaluate the RSC formulation. The TriHex™ was provided as dry powder. A total of 40mg of the TriHex™ powder was dissolved in 1mL (40mg/mL) of PBS at room temperature. Eight serial dilutions were prepared (100µg/mL, 50µg/mL, 25µg/mL, 12.5µg/mL, 6.25µg/mL, 3.125µg/mL, 1.5625µg/mL, and 0.78125µg/mL) to evaluate the toxicity of TriHex™. Twenty-four hours after seeding the cells, they were washed with PBS and treated with a serial dilution of the RSC formulation in cell culture media (fibroblast medium kit). Each condition was tested in triplicates. For the positive and negative controls, 8mM methyl methanesulfonate (MMS) and DMSO 100% were used, respectively.

Following the addition of the RSC formulation or TriHex™, the plates were incubated for 72 hours and one week, and the medium with the treatment was changed every two days. After the treatment period, the cells were washed with PBS twice, and the media was replaced with the MTT reagent at 0.5mg/mL in DMEM without phenol red. The plates were gently shaken and incubated for four hours. After the incubation, the medium was removed and replaced by DMSO. The plates were gently shaken to solubilize the formazan crystals. Absorbance was measured using an Envision multiplate reader (Perkin Elmer, Waltham, Massachusetts) at a wavelength of 570nm.

**Cell proliferation assessment.** Primary adult or neonatal human fibroblasts were cultured as described above. The culture medium was renewed every 2 to 3 days, and the cells were passaged at sub-confluence (70–80%) every seven days. The compounds (RSC at 500, 125, and 31.25µg/mL; TriHex™ at 3, 50, or 100µg/mL) or vehicle control were added to the cells in culture. Cell growth was monitored for each condition by counting the cell number at each passage using a Countess™ cell counter (Invitrogen). The population doubling (PD) value was calculated with the formula  $PD = 3.322(\log(C_f) - \log(C_i)) + x$  (C<sub>f</sub>: Final concentration; C<sub>i</sub>: initial concentration; X: PD last passage). One PD is equivalent to one round of cell replication.

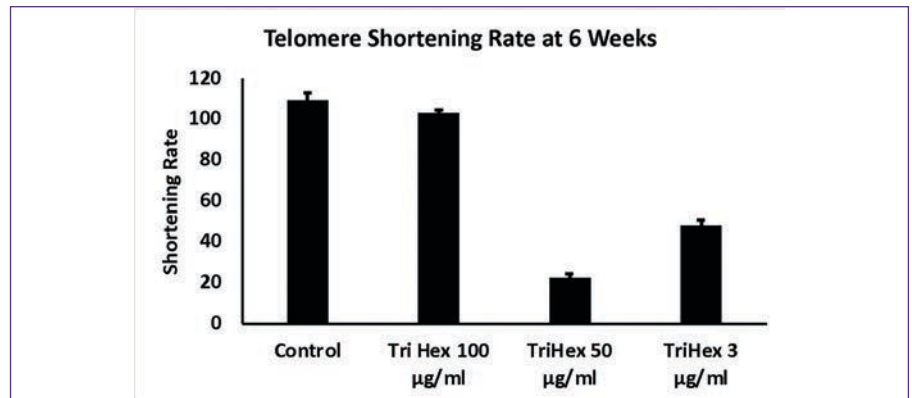


**FIGURE 3.** TriHex™ protects against telomere shortening in fibroblasts. Human primary neonatal fibroblasts were treated with the RSC formulation at 100, 50, and 3µg/mL for six weeks. The TAT assay was conducted to determine the telomere lengths. Then, the telomere shortening rate was determined by the following formula: median telomere length (initial-final)/population doubling. The values were compared, and the data represent the mean±SD. \*\*\*\*  $p < 0.0001$

### Telomere length assessment (TAT Assay).

Telomere length was determined using TAT, a method developed by Life Length, which uses a high-throughput (HT) quantitative fluorescent *in situ* hybridization (Q-FISH) technique. This method is based on a Q-FISH method modified for cells in interphase. Briefly, telomeres are hybridized with a fluorescent Peptide Nucleic Acid probe (PNA) that recognizes three telomere repeats (sequence: Alexa488-00-3CT1003CT1003CT100, Panagene). A High Content Screening Opera Phenix System (Perkin Elmer) captured the nuclei and telomeres images of the nuclei and telomeres using the Columbus software, Version 2.9 (PerkinElmer, Waltham, Massachusetts). The intensity of the fluorescent signal from the telomeric PNA probes that hybridize to a given telomere is proportional to the length of that telomere. The fluorescence intensities were translated to base pairs through a standard regression curve, which is generated using control cell lines with known telomere lengths.

To assess telomere length, primary adult or neonatal human fibroblasts were cultured as described above. The culture medium was renewed every 2 to 3 days, and the cells were passaged at sub-confluence (70–80%) every seven days. The compounds (RSC at 500, 125, and 31.25µg/mL; TriHex™ at 3, 50, or 100µg/mL) or vehicle control were added to the cells in culture. The cells were frozen in liquid nitrogen at Weeks 2, 4, 6, and 8. For the analysis, the cells were thawed at 37°C, and cell count and cellular viability were determined using a cell counter and the trypan blue exclusion method,

respectively. Viability lower than 60% was considered below our quality control standards, and these cells were not further analyzed. The cells were then seeded in clear-bottom, black-walled, 384-well plates at the density of 15,000 cells per well with five replicates for each experimental condition and eight replicates of each control. Two identical independent plates were prepared for each set of samples. The cells were fixed with methanol/acetic acid (3/1, vol/vol), treated with pepsin to digest the cytoplasm, and the nuclei were processed for *in situ* hybridization with the PNA probe. After several washing steps following standard DAPI incubation for DNA staining, the wells were filled up with mounting medium, and the plate was stored overnight at 4°C.

Images were captured using a 40x0.95 NA water immersion objective. UV and 488nm excitation wavelengths were used to detect the DAPI and A488 signals, respectively. With constant exposure settings, 15 independent images were captured at different positions for each well. Next, the nuclei images were used to define the region of interest for each cell, measuring the telomere fluorescence intensity of the A488 image for all of them. The intensity results for each focus were exported to the Columbus 2.4 software (Perkin Elmer). Life Length's proprietary program calculated the telomere length distribution, median telomere length distribution, and median telomere length.

**Clinical study.** The clinical study performed with the Restorative Skin Complex described above was reported in 2018.<sup>2</sup> The product was

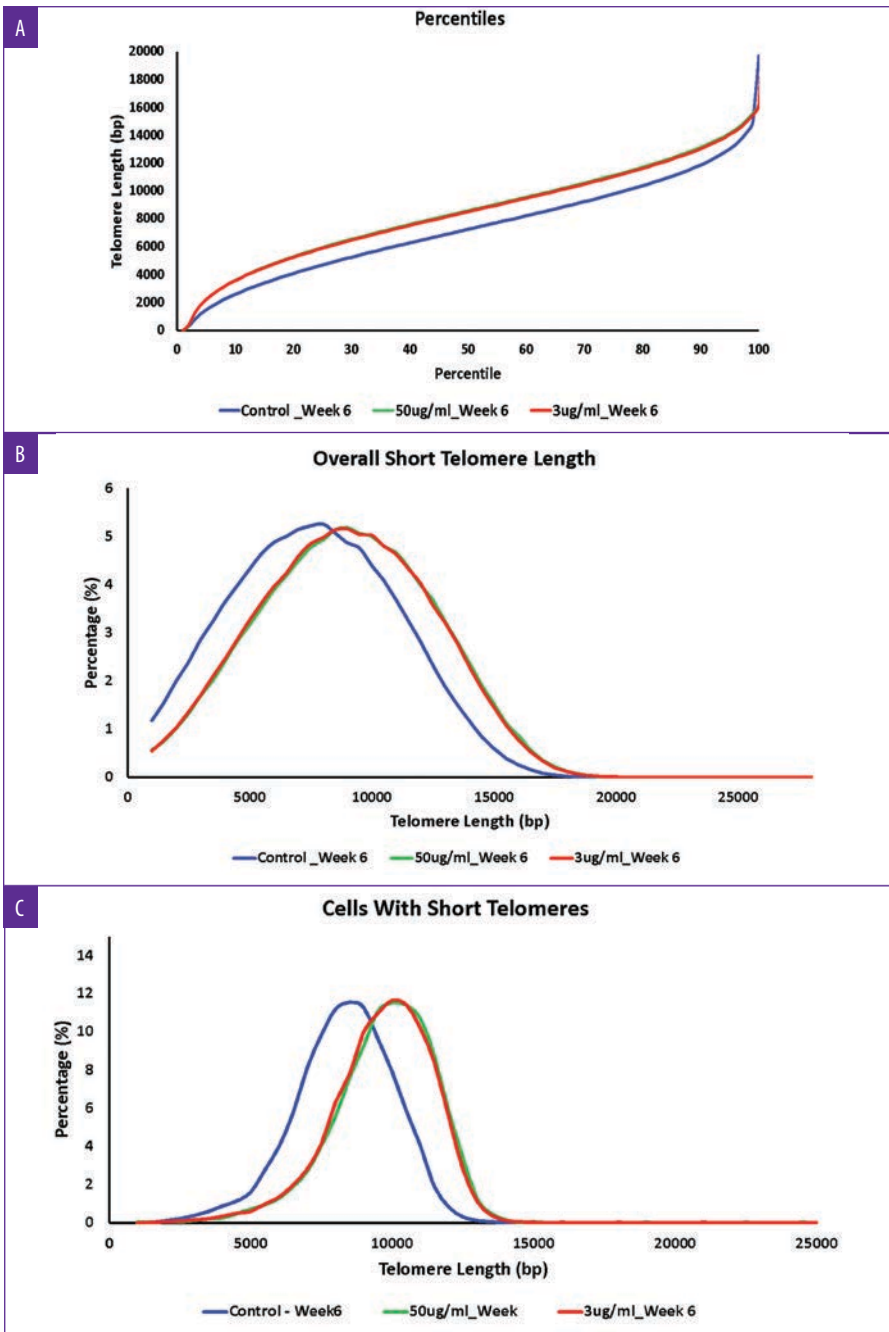


**FIGURE 4.** Full breakdown of telomere length distribution for fibroblasts treated with TriHex™ for six weeks. Human primary neonatal fibroblasts were treated with the TriHex™ at 100, 50, and 3  $\mu\text{g}/\text{mL}$  for six weeks. The TAT assay was conducted to determine the telomere lengths. **A)** The telomere length percentiles are one hundred individual telomere length measurements per sample, including the shortest telomeres' length (1st percentile length) and the length of the longest telomeres (100th percentile length). The percentiles allow for a comprehensive comparison between all the telomere lengths present in each sample throughout the telomere length distribution. **B)** The overall short telomere length variables are the percentages of telomeres with a specific telomere length. The variables identify whether one sample has a higher percentage (quantity) of shorter or longer telomeres and detect differences between samples in a specific area of the distribution. **C)** The assessment of cells with short telomere variables are the percentages of cells with a specific average telomere length. Since senescence and cell apoptosis affect the cells, this value addresses the telomeric profile on a cellular level. This value detected whether a sample presents a higher percentage of cells with shorter telomeres (closer to senescence) or longer ones.

tested among 22 subjects over the course of 12 weeks to assess its efficacy in women with mild to moderate wrinkles and skin sagging on the face. The efficacy of the product was assessed using investigator clinical grading measurements, raking light imaging, 3D imaging, biopsies, and self-assessment questionnaires at baseline and Weeks 4, 8, and 12.<sup>2</sup>

**Biopsy staining.** The biopsy specimens were examined by an experienced dermatopathologist to evaluate the staining. Five-micron thick tissue sections were stained with routine hematoxylin and eosin (HE). In addition, Movat pentachrome staining was used to evaluate elastin. Immunohistochemical staining for CD44 and fibrillin was performed by an automated stainer (Ventana Benchmark Ultra). All histological and immunohistochemical staining was performed with corresponding positive and negative controls.

## RESULTS

**RNA-seq investigation into Klotho and its related genes.** The differentially expressed genes from the keratinocyte RNA-seq analysis were analyzed, revealing that the Klotho gene (KL) was significantly upregulated by TriHex™ (3.5-fold) (Figure 1). The Klotho protein is a receptor for fibroblast growth factor 23 (FGF23).<sup>9</sup> Klotho is required for the high-affinity binding of FGF23 to its receptor FGFR1.<sup>10</sup> TriHex™ also significantly upregulated FGF23 and FGFR1 (4.1-fold and 6.3-fold, respectively) (Figure 1).

Klotho suppresses insulin/IGF-1 signaling and activates Forkhead box O (FOXO) proteins by inhibiting their phosphorylation, promoting their nuclear translocation.<sup>11</sup> Nuclear FOXO then directly binds to the MnSOD promoter and upregulates its expression, promoting antioxidant protection.<sup>12</sup> FOXO3 prolongs lifespan in *C. elegans* by regulating IGF-1 signaling.<sup>13</sup> FOXO3B was significantly upregulated by TriHex™ (2.5-fold) (Figure 1). In conclusion, TriHex™ stimulation induced keratinocytes to overexpress Klotho and other aging-related genes.

**Telomere investigation: Toxicity and proliferation assessments.** To prepare for the TAT assay, the toxicity and proliferative effects of the RSC formulation or TriHex™ on human adult or neonatal primary fibroblasts were determined, respectively. The MTT assay

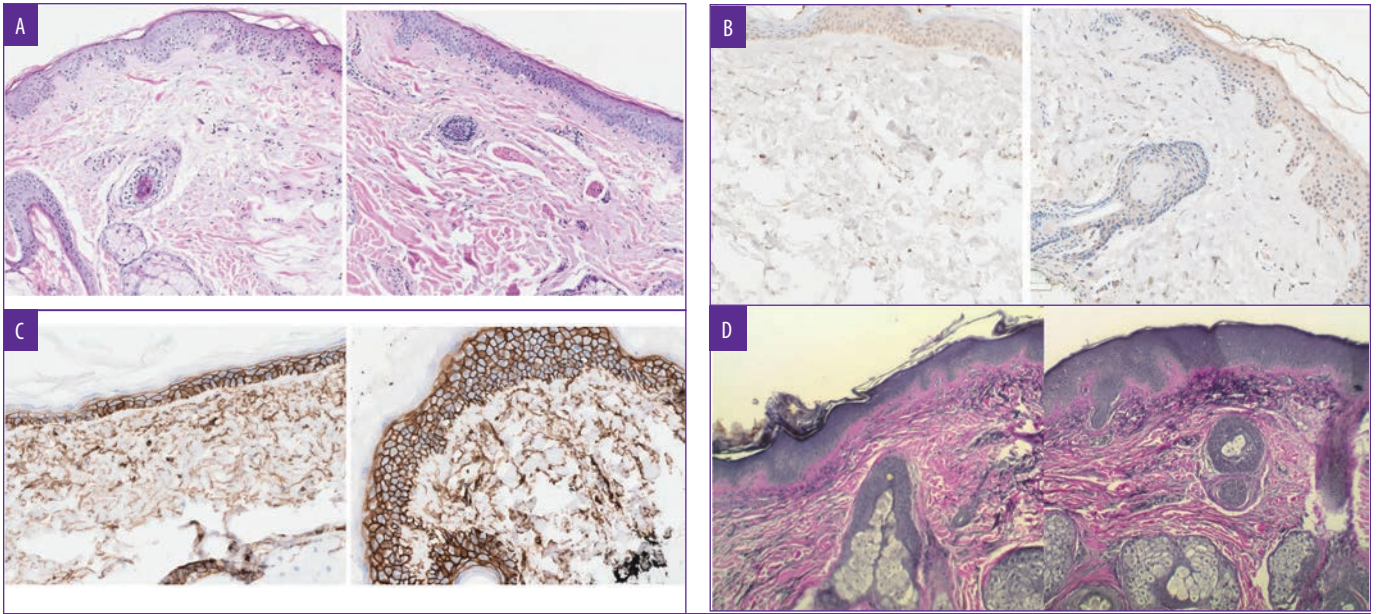


**FIGURE 5.** Biopsy staining showing anti-aging effects of RSC was tested among 22 subjects over the course of 12 weeks to assess its efficacy in women with mild to moderate wrinkles and skin sagging on the face. **A)** hematoxylin and eosin (HE) staining (100X) demonstrating changes in extracellular matrix (ECM) eight weeks following application; Figure 5A, right side, shows decreased solar elastosis, increased collagen in the papillary dermis and healthier ECM. **B)** Fibrillin (IHC) Figure 5B, right side, shows increased fibrillin within fibroblasts in the ECM. **C)** CD44 staining by IHC showing surface receptor staining for hyaluronic acid stimulation; Figure 5C, right side, shows increased levels in the dermis and epidermis. **D)** Movat stain for elastin; Figure 5D, right side, demonstrates increased elastin fiber stimulation in the papillary dermis and in the depths of the reticular dermis after eight weeks.

revealed that the ED50 (median effective dose) of the cells treated with the highest concentration of the RSC formulation (500 $\mu$ g/mL) was greater than 500 $\mu$ g/mL after 72 hours and one week. The TriHex™ ED50 (100  $\mu$ g/mL) was greater than 100  $\mu$ g/mL after 72 hours and one week of treatment. In addition, a morphological analysis using optical microscopy visualization (20x) did not show any deleterious effect at any concentration for both treatments, and no compound precipitation was observed at the concentrations tested. Thus, for the TAT assay concentrations of 500, 125, and 31.25  $\mu$ g/mL were selected for the RSC formulation, and 100, 50, and 3 $\mu$ g/mL were selected for TriHex™. The cumulative population doubling per passage (average of three measurements) over eight weeks for the RSC formulation showed a dose-dependent decrease in proliferation, and TriHex™ did not have a proliferative effect on the fibroblasts (Table 1).

**TAT analysis quality control.** Before conducting the TAT analysis, the cell count and viability of the cells used for the assay were determined. All the conditions and replicates showed adequate counts for the assay, and the viability average and standard deviation were 96.5% $\pm$ 4.1 for the RSC formulation and

**TABLE 1.** Assessment of population doubling over eight weeks after RSC and TriHex™ treatment

Week	1	2	3	4	5	6	7	8
Control RSC	3.5	7.23	10.21	13.2	16.6	19.61	22.35	24.94
RSC 500 $\mu$ g/mL	3.48	6.35	7.84	9.02	10.1	11.34	11.65	12.35
RSC 125 $\mu$ g/mL	3.44	6.87	9.32	12.27	14.92	17.27	19.23	21.43
RSC 31.25 $\mu$ g/mL	3.37	6.73	9.19	12.26	15.3	18.49	20.93	23.61
Control TriHex™	3.52	6.89	10.06	13.2	16.17	19.49	22.01	24.76
TriHex™ 100 $\mu$ g/mL	3.59	7.19	10.5	13.57	16.67	19.89	21.42	23.9
TriHex™ 50 $\mu$ g/mL	3.56	7.13	10.2	13.21	16.14	19.32	21.81	24.46
TriHex™ 3 $\mu$ g/mL	3.59	7.29	10.55	13.38	16.01	19.06	21.3	23.71

96.1% $\pm$ 3.2 for TriHex™. Thus, the quality control parameters were met to proceed with the TAT analysis.

**RSC formulation TAT analysis.** The TAT analysis produced the median telomere length (base pairs (bp)), the 20th percentile telomere length (bp), and the percentage of telomeres shorter than 3kbp in the different time points and treatments. To extrapolate the significance of these data, we had to consider that cell replication is one of the principal causes of telomere shortening.<sup>14</sup> Thus, the telomere length measurements were normalized based on the population doubling values (cell replication) for each condition and time point. The values obtained were the

telomere shortening rates (median telomere length (initial-final)/population doubling) at the defined time points and treatments. The change in telomere shortening rate of the cells treated with the RSC formulation at 125 $\mu$ g/mL at four weeks showed a significant reduction in telomere shortening rate compared to the control ( $p < 0.05$ ) (Figure 2). Based on our gene expression studies, we hypothesized that the TriHex™ component of the RSC formulation contributed to the telomere protection. Thus, we analyzed cells treated with TriHex™ in greater detail to assess the telomere effects.

**TriHex™ TAT analysis.** The median telomere length (bp), the 20th percentile telomere length (bp), and the percentage of telomeres

**TABLE 2.** Summary of TAT Analysis after TriHex™ Treatment Human fibroblasts were treated with TriHex™ as indicated. (bp=base pairs; CV=coefficient of variation).

TREATMENT AND TIMEPOINT	MEDIAN LENGTH (BP)	20TH PERCENTILE LENGTH (BP)	TELOMERES <3KBP (%)	CV (%)
Control-Week 0	9,632	6,737	2.97	2.25
Control-Week 2	10,163	7,251	2.05	0.37
100µg/mL Week 2	10,114	7,187	2.22	2.58
50µg/mL Week 2	10,147	7,225	2.25	1.19
3µg/mL Week 2	9,926	6,965	2.7	3.6
Control-Week 4	8,817	5,717	5.67	4.27
100µg/mL Week 4	8,727	5,630	6.07	4.16
50µg/mL Week 4	9,044	5,967	5.03	3.94
3µg/mL Week 4	8,809	5,679	5.78	1.48
Control-Week 6	7,492	4,329	11.04	3.21
100µg/mL Week 6	7,579	4,383	10.9	1.6
50µg/mL Week 6	9,181	5,978	5.12	1.46
3µg/mL Week 6	8,707	5,486	6.28	2.57
Control-Week 8	8,552	5,237	8.17	0.85
100µg/mL Week 8	8,409	5,100	8.31	1.9
50µg/mL Week 8	8,585	5,321	7.51	4.8
3µg/mL Week 8	8,433	5,171	7.9	4.19

**TABLE 3.** Telomere Shortening Rate

TREATMENT	WEEK 2	WEEK 4	WEEK 6	WEEK 8
Control	-74.9	62.6	109.8	43.6
TriHex™ 100µg/mL	-67.7	66.3	103.2	51.7
TriHex™ 50µg/mL	-73.9	43.1	23	43
TriHex™ 3µg/mL	-40.5	61.4	48.4	50.8

shorter than 3kbp in the different timepoints and treatments are presented in Table 2 with the coefficient of variation (CV%). The telomere shortening rates were then determined at the defined time points and treatments (Table 3). The change in telomere shortening rate of the cells treated with the TriHex™ formulation at 50 and 3µg/mL at six weeks showed a significant reduction in telomere shortening rate compared to the control ( $p < 0.001$ ) (Figure 3). Thus, we analyzed these treatments and timepoint in greater detail.

First, as determined by HT-QFISH, the telomere length distributions were assessed based on the percentile value, which indicates the telomere length in base pairs for each one of the percentiles in the telomere length distribution of each sample. For instance, for the telomere length distributions, a 20th percentile of 6,700 base pairs indicates that 20 percent of the telomeres in the sample have lengths below 6,700 base pairs. The data revealed that

treatment with TriHex™ at 50 and 3µg/mL at six weeks showed statistically significantly longer telomere lengths for all percentiles than the control (Figure 4A).

Next, we examined the number of short telomeres per group, ranging in length from 1000bp to 35000bp, and the percentile was calculated based on increments of 500bp. Based on the histogram, the greatest percentile for all the groups was approximately five percent. However, for the control, this percentile showed an average length of 7500 to 8000bp compared to 8500 to 9000bp for the TriHex™ treatment at 50 and 3µg/mL (Figure 4B). Thus, the size of the short telomeres was longer after the TriHex™ treatment.

Finally, we assessed short telomere lengths ranging from 1000bp to 35000bp at the cellular level, meaning the average telomere length per cell. All the groups maxed at approximately 12 percent for the cell percentage based on the histogram. For the control, the telomere length

most represented by that population of cells was 8000 to 8500bp compared to 10000 to 10500 for the cells treated with TriHex™ at 50 and 3µg/mL (Figure 4C). These data reveal that treatment with TriHex™ produced a higher quantity of cells with longer telomeres.

**Results of clinical study 2.** The results of this study have been previously published.<sup>2</sup> Assessment by clinical grading indicated that use of the antiaging regimen for 12 weeks produced a statistically significant improvement in scores for all evaluated parameters. The raking light image analysis demonstrated a statistically significant improvement in values for length, width, and area of wrinkles when compared with baseline values as did 3D imaging. Results from the self-assessment questionnaire analysis indicated favorable responses in a statistically significant proportion of subjects after 12 weeks of use for all inquiries. It was concluded that the use of this facial antiaging regimen was effective in improving visual facial photoaging conditions and well-perceived when used by women with mild to moderate wrinkles and skin sagging on the face under the conditions of the study.<sup>2</sup>

**Biopsy: histology.** Biopsy results in the five patients tested in the original trial showed improvement in solar elastosis, collagen stimulation, and improvement in cornified layers in all five patients. Elastin stimulation was evident in three of five patients.<sup>2</sup> Restaining of the slides from the original study with additional stains confirmed improvement in solar elastosis by H&E staining (Figure 5A), the right demonstrates increased elastin fiber stimulation in the papillary dermis and in the depths of the reticular dermis after eight weeks.

## DISCUSSION

The RSC formulation was tested among a group of 22 subjects over the course of 12 weeks to assess its efficacy in women with mild to moderate wrinkles and skin sagging on the face. Results were published as reported above. While well-designed clinical studies are the gold standard for assessing topical product efficacy, it is important to delve deeper into mechanistic pathways and gene regulation to explain this efficacy. This study examined new areas of anti-aging science that are being explored in more recent literature.<sup>5-7, 15</sup>

Aging and longevity are determined by a complex combination of genetic, nongenetic,

and environmental factors. Klotho and other genes have been demonstrated to be associated with life extension and in animal models. Gene mutations causing decreased Klotho expression dramatically decrease the lifespan in mice. Klotho genes are now considered potential targets for interventions of aging impacting human longevity.<sup>5,6,16</sup> Klotho is one of the most well-studied genes for extension of life in many animal models. Klotho overexpression has profound effects on proliferation, oxidation, senescence, autophagy, and modulation of insulin, TGF- $\beta$ , and Wnt signaling pathways. Klotho deficiency activates Wnt expression and contributes to the senescence and depletion of stem cells, which consequently triggers tissue atrophy and fibrosis.<sup>7</sup>

Part of the mechanism by which Klotho functions as an anti-aging gene can be understood by examining its signal transduction. Klotho shows high-affinity binding to FGF23, which is required for binding and signaling through FGFR.<sup>20,11</sup> The activation of this signal transduction suppresses the autophosphorylation of insulin/IGF-1 receptors and downstream signaling events, including the tyrosine phosphorylation of insulin receptor substrates (IRS) and phosphoinositide 3-kinase (PI3K) p85 association with IRS proteins. Inhibition of the insulin/IGF-1/PI3K signaling by Klotho suppresses aging by inducing resistance to oxidative stress.<sup>17</sup> The insulin/IGF-1/PI3K pathway is linked to oxidative stress via the FoxO forkhead transcription factors (FOXOs). Upon suppression of the insulin/IGF-1/PI3K pathway, FOXO3, a longevity factor, is free to activate the transcription of targets that regulate aging.<sup>18</sup> By RNA-seq, we revealed that TriHex™ triggered the upregulation of Klotho, FGFR1, FGF23, and FOXO3 in keratinocytes. Klotho protein has been suggested as an ideal therapy to eliminate UVB-induced cell damage, such as actinic keratosis, through the reversal of the NF- $\kappa$ B stimulated UVB-induced damage to keratinocyte cells.<sup>6</sup> Thus, increased Klotho, FGFR1, FGF23, and FOXO3 keratinocyte expression would provide a major boost to an anti-aging formulation limiting UV-related skin damage and providing optimized health to these cells.

The oxidative stress protection offered via the Klotho and FOXO3 contributes to their role in longevity, but they are also known to regulate telomere length and activity.<sup>19,20</sup> Telomeres are dynamic DNA-protein complexes

that protect the ends of chromosomes and promote chromosomal stability. When cells divide, telomeres are not fully replicated, leading to telomere shortening with every replication. Once telomeres become critically short, cells stop dividing and enter senescence. Thus, telomere length is considered a marker of cellular aging. Telomerase is the enzyme responsible for adding DNA sequences to the ends of telomeres and maintaining their length.<sup>21</sup>

Stem cells in conjugation with anti-aging genes probably receive and neutralize most of the devastating signaling effects known to cause premature aging. However, this is just one potential pathway in a complex anti-aging journey.<sup>7</sup> When telomeres in mice are made to progressively shorten, these animals age much faster than normal mice. In addition, conditions that trigger premature aging, such as telomere shortening, also impair the ability of stem cells to regenerate tissues. Short telomeres increase the likelihood of cells becoming senescent and producing molecules that lead to inflammation, which is a huge risk factor for age-related diseases.<sup>7</sup> Thus, stem cells, together with anti-aging genes such as Klotho and FOXO3, play a crucial role in delaying the aging process.

Fibroblasts are responsible for collagen synthesis, fibril formation, ECM integrity, and skin aging. However, with time, wear and tear, and oxidative damage, fibroblasts become senescent. As fibroblasts age, their telomere length decreases, and the senescent cells secrete inflammatory mediators, and cumulative damage results in loss of functional ECM and subsequent aging.<sup>7</sup> Thus, finding new bioactives to impede telomere loss or repair DNA damage is a new area of research that may offer new treatments in the fight against skin aging.<sup>22</sup>

Having the dual action of telomere length protection and Klotho and FOXO3 gene upregulation, the TriHex™ technology and the RSC formulation are well placed in the anti-aging armamentarium. Moreover, the demonstration of clinical efficacy while at the same time delineating the mechanisms of the biological activity at a molecular level provides excellent all-around validation of the anti-aging function of the formulation and its peptides. While oxidative stress accelerates telomere erosion, antioxidants may decelerate it. One of these anti-oxidants in the RSC formulation is ergothioneine, a naturally occurring amino acid

synthesized exclusively by fungi, cyanobacteria, and mycobacteria.<sup>21</sup> Studies have demonstrated that ergothioneine exerts a protective effect on telomeres, especially under oxidative conditions.<sup>21</sup> It may have sufficed to assume that the RSC formulation produced its preventative effects on telomere shortening through the addition of ergothioneine as a component. However, the demonstration of an additive, if not increased effect of TriHex™ not only on telomere length protection, but also as an upregulator of the Klotho and FOXO3 genes, provides excellent validation for the anti-aging efficacy of the RSC formulation and the TriHex™ combination in general. It is noteworthy that the synergy of these two peptides is what provides the "Klotho and FOXO3 effect" as opposed to the action of the peptides alone.

Finally, validation of transcription and subsequent translation of protein production is best provided by histological validation of product efficacy. In this study, ECM remodeling, new collagen and elastin formation, and the stimulation of hyaluronic acid production provided proof of the formulation's multilayer regenerative rejuvenating effect.

## CONCLUSION

The term "anti-aging" is used very loosely and commonly when describing new topical preparations that purport to support skin health. It is important that this description is accompanied by the relevant science to validate such a claim. With a newer understanding of the biological mechanisms involved in combatting skin cellular aging, it is imperative that these mechanisms are explored in studies related to the efficacy of formulations. Thus, clinical studies demonstrating good outcomes are essential but tracking the effect of these topicals on telomere shortening, epigenetic and genetic investigations, such as the newly described Klotho and FOXO3 genes, and biopsy validation provide a comprehensive validation of anti-aging efficacy. The TriHex™ technology and the RSC formulation have been demonstrated to significantly impact all these described areas providing excellent proof of efficacy.

## REFERENCES

1. Widgerow AD, Fabi SG, Palestine RF, et al. Extracellular Matrix Modulation: Optimizing Skin Care and Rejuvenation Procedures. *Journal of drugs in dermatology*. 2016;15(4s):S63–S71.

2. Widgerow AD, Jiang LI, Calame A. A single-center clinical trial to evaluate the efficacy of a tripeptide/hexapeptide antiaging regimen. *J Cosmet Dermatol*. 2018. Epub 2018/03/06.
3. Calame A, Widgerow A. Histological Changes Associated with Extracellular Matrix-Remodeling Topical Therapy. *Dermatology Case Reports*. 2017;2(2):1000126.
4. Widgerow AD, Cohen SR, Fagien S. Preoperative Skin Conditioning: Extracellular Matrix Clearance and Skin Bed Preparation, A New Paradigm. *Aesthetic Surgery Journal*. 2019;39(Supplement\_3):S103–S111.
5. Kuro-o M. Klotho and aging. *Biochimica et biophysica acta*. 2009;1790(10):1049–1058. Epub 2009/02/24.
6. Zhang B, Xu J, Quan Z, et al. Klotho Protein Protects Human Keratinocytes from UVB-Induced Damage Possibly by Reducing Expression and Nuclear Translocation of NF-kappaB. *Med Sci Monit*. 2018;24:8583–8591. Epub 2018/11/28.
7. Ullah M, Sun Z. Stem cells and anti-aging genes: double-edged sword-do the same job of life extension. *Stem Cell Res Ther*. 2018;9(1):3.
8. Griss J, Guilherme V, Konstantinos S, et al. Efficient Multi-Omics Comparative Pathway Analysis. *Mol Cell Proteomics*. 2020;19(12):2115–2125.
9. Shimada T, Kakitani M, Yamazaki Y, et al. Targeted ablation of Fgf23 demonstrates an essential physiological role of FGF23 in phosphate and vitamin D metabolism. *Journal of Clinical Investigation*. 2004;113(4):561–568.
10. Chen G, Liu Y, Goetz R, et al. alpha-Klotho is a non-enzymatic molecular scaffold for FGF23 hormone signalling. *Nature*. 2018;553(7689):461–466. Epub 2018/01/18.
11. Yamamoto M, Clark J, Pastor J, et al. Regulation of Oxidative Stress by the Anti-aging Hormone Klotho. *The Journal of biological chemistry*. 2005;280(45):38029–38034.
12. Lim SW, Jin L, Luo K, et al. Klotho enhances FoxO3-mediated manganese superoxide dismutase expression by negatively regulating PI3K/AKT pathway during tacrolimus-induced oxidative stress. *Cell Death Dis*. 2017;8(8):e2972. Epub 2017/08/05.
13. Ogg S, Paradis S, Gottlieb S, et al. The Fork head transcription factor DAF-16 transduces insulin-like metabolic and longevity signals in *C. elegans*. *Nature*. 1997;389(6654):994–999.
14. Shammass MA. Telomeres, lifestyle, cancer, and aging. *Curr Opin Clin Nutr Metab Care*. 2011;14(1):28–34. Epub 2010/11/26.
15. Yamashita K, Yotsuyanagi T, Yamauchi M, et al. Klotho mice: a novel wound model of aged skin. *Plastic and reconstructive surgery Global open*. 2014;2(1):e101. Epub 2014/10/08.
16. Dermaku-Sopjani M, Kolgeci S, Abazi S, et al. Significance of the anti-aging protein Klotho. *Mol Membr Biol*. 2013;30(8):369–385. Epub 2013/10/16.
17. Kenyon C. The plasticity of aging: insights from long-lived mutants. *Cell*. 2005;120(4):449–460. Epub 2005/03/01.
18. Martins R, Lithgow GJ, Link W. Long live FOXO: unraveling the role of FOXO proteins in aging and longevity. *Aging Cell*. 2016;15(2):196–207.
19. Ullah M, Sun Z. Klotho Deficiency Accelerates Stem Cells Aging by Impairing Telomerase Activity. *J Gerontol A Biol Sci Med Sci*. 2019;74(9):139w6–1407.
20. Allsopp R, Davy P, Willcox C, et al. The Longevity Associated Allele Of Foxo3 Protects Against Telomere Attrition During Aging. *Innov Aging*. 2019;3(Suppl 1):S99–S100.
21. Samuel P, Tsapekos M, de Pedro N, et al. Ergothioneine Mitigates Telomere Shortening under Oxidative Stress Conditions. *J Diet Suppl*. 2020;1-14. Epub 2020/12/09.
22. Reilly DM, Lozano J. Skin collagen through the lifestages: importance for skin health and beauty. *Plastic and Aesthetic Research*. 2021.

**JCAD**